

How To Make A Thesis Following The Guideline With More Text To Have Two Lines



by

A Good Name

Submitted for the degree of

Doctor of Philosophy

SOME WEIRD INSTITUTE NO ONE EVER HEARD ABOUT

SCHOOL OF LATEX AND WRITING

HERIOT-WATT UNIVERSITY

September 2042

Abstract

In accordance with the Academic Regulations the thesis must contain an abstract preferably not exceeding 200 words, bound in to precede the thesis. The abstract should appear on its own, on a single page. The format should be the same as that of the main text. The abstract should provide a synopsis of the thesis and shall state clearly the nature and scope of the research undertaken and of the contribution made to the knowledge of the subject treated. There should be a brief statement of the method of investigation where appropriate, an outline of the major divisions or principal arguments of the work and a summary of any conclusions reached. The abstract must follow the Title Page.

Dedication

If a dedication is included then it should be immediately after the Abstract page.

I don't what it is actually.

Acknowledgements

I wanna thanks all coffee and tea manufacturers and sellers that made the completion of this work possible.

Contents

I	Chapters	1
1	Introduction	2
1.1	Paragraph 4: Synergistic Challenges in Applications Prone to Corrosion and Cavitation IGNORE	6
1.2	Paragraph 5: Research and Development for Enhanced Corrosion and Cavitation Performance IGNORE	6
1.3	Paragraph 6: Influence of HIPing IGNORE	6
1.4	Paragraph: Cavitation Erosion Resistance	6
1.5	General Background	6
1.6	Stellite 1	8
1.7	Stellites	8
1.8	Objectives and Scope of the Research Work	8
1.9	Thesis Outline	8
1.10	Literature Survey	8
1.11	Cavitation Tests	8
2	Analytical Investigations	9
2.1	Strain hardening	9
2.2	Correlative empirical methods	9
3	Experimental Investigations	12
3.1	Materials and Microstructure	12
4	Discussion	13
4.1	Experimental Test Procedure	13
4.1.1	Hardness Tests	13
4.1.2	Cavitation	13
4.2	Relationships between cavitation erosion resistance and mechanical properties . .	13
4.3	Influence of vibratory amplitude	13
	References	14

List of Tables

List of Figures

Glossary

BSE Backscatter Electrons.

EDX Energy-Dispersive X-ray.

FCC Face Centred Cubic.

HCP Hexagonal Close Packed.

HIP Hot Isostatically Pressed.

HV Hardness Vickers Scale.

PDF Powder Diffraction File.

SE Secondary Electrons.

SEM Scanning Electron Microscope/Microscopy.

XRD X-ray Diffraction.

Part I

Chapters

Chapter 1

Introduction

Stellites are cobalt-base superalloys used in aggressive service environments due to retention of strength, wear resistance, and oxidation resistance at high temperature [1, 2]. Originating with Elwood Haynes's development of alloys like Stellite 6 in the early 1900s [3], stellites quickly found use in medical implants & tools, machine tools, and nuclear components, and new variations on the original CoCrWC and CoCrMoC alloys are spreading to new sectors like oil & gas and chemical processing [1, 4, 5].

The main alloying elements in Stellite alloys are cobalt (Co), chromium (25-33 wt% Cr), tungsten (0-18 wt% W), molybdenum (0-18 wt% Mo), carbon (0.1-3.3 wt% C), and trace elements iron (Fe), nickel (Ni), silicon (Si), phosphorus (P), sulphur (S), boron (B), lanthanum (La), & manganese (Mn); Table 1 summarizes the nominal and measured composition of commonly used Stellite alloys [6–15]. Stellite alloys possess a composite-like microstructure, combining a cobalt-rich matrix strengthened by solid solutions of chromium, tungsten, & molybdenum, with hard carbide phases with carbide formers Cr (of carbide type M_7C_3 & $M_{23}C_6$) and W/Mo (of carbide type MC & M_6C), that impede wear and crack propagation [16, 17]. The proportion and type of carbides depend on carbon content and the relative amounts of carbon with carbide formers (Cr, W, Mo), which greatly influence alloy performance and intended applications; high carbon alloy (>1.2 wt%) have greater carbide formation and are primarily used for wear resistance, low carbon alloys (<0.5 wt%) are used for enhanced corrosion resistance, while medium carbon alloys (0.5 wt% - 1.2 wt%) are used in applications requiring a combination of wear and corrosion resistance [10].

The Co solid solution in Stellites is a metastable fcc crystal with a very low stacking fault energy.

[10, 18]

Tungsten (W) and molybdenum (Mo) serve to provide additional strength to the matrix, when present in a small amount (<4 wt%), by virtue of their large atomic size that impedes dislocation flow when present as solute atoms. When present in large quantities, W and Mo also participate in formation of W-rich or Mo-rich carbides during alloy solidification

[10] [5]

There are two main phases in the tungsten-carbon system: the hexagonal WC (ICDD Card# 03-065-4539, COD:2102265), denoted as δ – WC, and multiple variations of hexagonal-close-

Alloy	Co	Cr	W	Mo	C	Fe	Ni	Si	P	S	B	La	Mn	Ref	Process Type	Observation
Stellite 1	47.7	30	13	0.5	2.5	3	1.5	1.3					0.5	[10]	Nominal composition	
	48.6	33	12.5	0	2.5	1	1	1.3					0.1	[7]		
	46.84	31.7	12.7	0.29	2.47	2.3	2.38	1.06					0.26	[6]	HIPed	ICP-OES
Stellite 3	50.5	33	14		2.5									[9]		
	49.24	29.57	12.07	0.67	2.52	2.32	1.07	1.79					0.75	[14]	HIPed	ICP-OES
Stellite 4	45.43	30	14	1	0.57	3	3	2					1	[10]	Nominal composition	
	51.5	30	14		1	1	2	0.5						[15]		
	51.9	33	14		1.1									[9]		
	49.41	31	14	0.12	0.67	2.16	1.82	1.04					0.26	[6]	HIPed	ICP-OES
	50.2	29.8	14.4	0	0.7	1.9	1.9	0.8					0.3	[8]	HIPed	
Stellite 6	51.5	28.5	4.5	1.5	1	5	3	2			1		2	[10]	Nominal composition	
	63.81	27.08	5.01		0.96	0.73	0.87	1.47					0.07	[14]	HIPed	ICP-OES
	60.3	29	4.5		1.2	2	2	1						[15]		
	61.7	27.5	4.5	0.5	1.15	1.5	1.5	1.15					0.5	[9]		
	58.46	29.5	4.6	0.22	1.09	2.09	2.45	1.32					0.27	[6]	HIPed	ICP-OES
	58.04	30.59	4.72		1.24	2.03	1.87	0.80	0.01	0.01				[12]	PTAW	OES
	55.95	27.85	3.29		0.87	6.24	3.63	1.23	0.01	0.01			0.45	[12]	GTAW	OES
	52.40	30.37	3.57		0.96	6.46	3.93	1.70	0.01	0.01			0.3	[12]	SMAW	OES

	60.3		31.10	4.70	0.30	1.10	1.70	1.50	1.30	0.00	0.3	[13]	LP-DED	ICP-AES & GDMS
	60.6	27.7	5	0	1.2	1.9	2	1.3			0.3	[8]	HIPed	
Stellite 12	53.6	30	8.3		1.4	3	1.5	0.7			1.5	[10]		Nominal composition
	55.22	29.65	8.15	0.2	1.49	2.07	2.04	0.91			0.27	[6]	HIPed	ICP-OES
Stellite 19	50.94	31.42	10.08	0.79	2.36	1.82	2	0.4		0.09	0.1	[11]		
Stellite 20	41.05	33	17.5		2.45	2.5	2.5				1	[10]		Nominal composition
	43.19	31.85	16.3	0.27	2.35	2.5	2.28	1			0.26	[6]	HIPed	ICP-OES
Stellite 21	59.493	27		5.5	0.25	3	2.75	1		0.007	1	[10]		Nominal composition
	60.6	26.9	0	5.7	0.2	1.3	2.7	1.9			0.7	[8]	HIPed	
Stellite 31	57.5	22	7.5		0.5	1.5	10	0.5			0.5	[10]		Nominal composition
	52.9	25.3	7.8	0	0.5	1.1	11.4	0.6			0.4	[8]	HIPed	
Stellite 190	46.7	27	14	1	3.3	3	3	1			1	[10]		Nominal composition
	48.72	27.25	14.4	0.2	3.21	2.1	2.81	1			0.31	[6]	HIPed	ICP-OES

Hot Isostatic Pressing

Inductively coupled plasma atomic emission spectroscopy

Shielded metal arc welding

Gas tungsten Arc Welding

Plasma transfered Arc Welding

packed $W_2\{C\}$ (ICDD:00-002-1134, COD:1539792) [19].

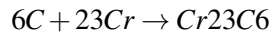
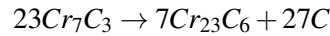
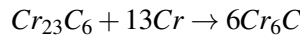
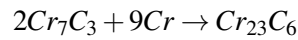
The precipitation of the tungsten-rich phase M_6C is closely related to the decomposition of the MC carbide, and the M_6C only occurs in the vicinity of the MC [20], as M_6C carbides form only when the tungsten and/or molybdenum content exceeds 4-6 a/o.

Although $M_{23}C_6$ can precipitate as primary carbide during solidification, it is most commonly found in secondary carbides along grain boundaries.

M_7C_3 is a metastable pseudo-eutectic carbide that typically forms at lower carbon-chromium ratios and effectively transforms into secondary $M_{23}C_6$ upon heat treatment.

In addition to being a carbide former, chromium provides solid solution strengthening and corrosion/oxidation resistance to the cobalt-based matrix.

The Cr_7C_3 carbide is unstable at high temperatures and transforms to $M_{23}C_6$ upon heat treatment. Under further temperature and time, $Cr_{23}C_6$ partially transforms to Cr_6C [21].



The remarkable ability of Stellite alloys to withstand these specific challenges stems from key metallurgical features. Their corrosion resistance is primarily attributed to a high chromium content, typically 20-30 wt.%, which promotes the formation of a highly stable, tenacious, and self-healing chromium-rich passive oxide film on the material's surface; this film acts as a barrier isolating the underlying alloy from the corrosive environment. Alloying elements such as molybdenum and tungsten can further enhance this passivity, particularly improving resistance to localized corrosion phenomena like pitting and crevice corrosion in aggressive media. Concurrently, their outstanding cavitation resistance is largely derived from the unique behavior of the cobalt-rich matrix, which can undergo a stress-induced crystallographic transformation from a face-centered cubic (fcc) to a hexagonal close-packed (hcp) structure. This transformation, often facilitated by mechanical twinning, effectively absorbs the intense, localized impact energy from collapsing cavitation bubbles and leads to significant work hardening, thereby impeding material detachment and erosion.

Antony suggests that the cavitation-erosion resistance of Stellites derives from the matrix phase and is enhanced by the strain-induced fcc \rightarrow hcp allotropic transformation [22].

The aqueous oxidation of Stellite 6 alloy was investigated in a 1979 study using X-ray Photo-

electron Spectroscopy (XPS) [23]. Specimens were exposed to pH 10 water at 285°C. To understand the oxidation behavior, the study measured dissolved oxygen concentration against exposure duration.

The high-temperature corrosion resistance of stellite coatings is attributable to the formation of cobalt & chromium surface [24].

Heathcock et al found that carbides are selectively eroded, with the carbide-matrix interface acting as initiating erosion site [25].

1.1 Paragraph 4: Synergistic Challenges in Applications Prone to Corrosion and Cavitation

IGNORE

1.2 Paragraph 5: Research and Development for Enhanced Corrosion and Cavitation Performance

IGNORE

1.3 Paragraph 6: Influence of HIPing

IGNORE

Compared with the case alloys, the HIPed alloys had relatively finer, rounded, and distributed carbides.

1.4 Paragraph: Cavitation Erosion Resistance

The primary result of an erosion test is the cumulative mass loss versus time, which is then converted to volumetric loss and mean depth of erosion (MDE) versus time for the purposes of comparison between materials of different densities. The calculation of the mean depth of erosion for this test method should be performed in conformity with ASTM G-32.

1.5 General Background

%cite:@Franc2004265, @Romo201216, @Kumar2024, @Kim200685, @Gao2024, @20221xix, @Usta2023, @Cheng2023, @Zheng2022

Cavitation erosion presents a significant challenge in materials degradation in various industrial sectors, including hydroelectric power, marine propulsion, and nuclear systems, stemming from a complex interaction between fluid dynamics and material response [26, 27]. Hydrodynamically, the phenomenon initiates with the formation and subsequent violent collapse of vapor bubbles within a liquid, triggered by local pressures dropping to the saturated vapor pressure. These implosions generate intense, localized shockwaves and high-speed microjets that repeat-

edly impact adjacent solid surfaces [28]. From a materials perspective, these impacts induce high stresses (100-1000 MPa) and high strain rates, surpassing material thresholds and leading to damage accumulation via plastic deformation, work hardening, fatigue crack initiation and propagation, and eventual material detachment. Mitigating this requires materials capable of effectively absorbing or resisting this dynamic loading, often under demanding conditions that may also include corrosion.

% Martensitic transformation Crucially, the cobalt matrix often possesses a low stacking fault energy, facilitating a strain-induced martensitic transformation from a metastable face-centered cubic γ phase to a hexagonal close-packed ϵ phase under the intense loading of cavitation. This transformation is a primary mechanism for dissipating impact energy and enhancing work hardening, contributing significantly to Stellite's characteristic cavitation resistance [29, 30].

HIPing is a thermo-mechanical material processing technique which involves the simultaneous application of pressure (up to 200 MPa) and temperature (2000 C), which results in casting densification, porosity closure, and metallurgical bonding. [31]

While commonly applied via casting or weld overlays, processing routes like Hot Isostatic Pressing (HIP) offer potential advantages such as microstructure refinement [32] finer microstructures and enhanced fatigue resistance [31, 33].

HIPing of surface coatings results in microstructure refinement, which can yield improved fatigue and fracture resistance.

HIPing leads to carbide refinement, which can yield improved impact toughness [34], and reduce carbide brittleness [31].

Furthermore, HIP facilitates the consolidation of novel 'blended' alloys created from mixed elemental or pre-alloyed powders, providing a pathway to potentially tailor compositions or microstructures for optimized performance. However, despite the prevalence of Stellite alloys and the known influence of processing on microstructure and properties, the specific cavitation erosion behavior of HIP-consolidated Stellites, particularly these blended formulations, remains underexplored in academic literature. Given that erosion mechanisms in Stellites often involve interactions at the carbide-matrix interface [35], understanding how HIP processing and compositional blending affect these interfaces and the matrix's transformative capacity under cavitation, especially when potentially coupled with corrosion, constitutes a critical knowledge gap addressed by this research.

% Need to describe Stellite 1

1.6 Stellite 1

Stellite 1 is a high-carbon and high-tungsten alloy, making it suitable for demanding applications that require hardness & toughness to combat sliding & abrasive wear [[17](#)]

1.7 Stellites

1.8 Objectives and Scope of the Research Work

1.9 Thesis Outline

1.10 Literature Survey

1.11 Cavitation Tests

Chapter 2

Analytical Investigations

2.1 Strain hardening

Cavitation bubble collapse induce a work hardening of the material surface, comparable to that obtained in conventional peening [36], characterized by the thickness of the hardened layers and the shape of the strain profile below the surface.

The strain profile within the material can usually be modeled by the following power law:

$$\varepsilon(x) = \varepsilon_s \left(1 - \frac{x}{L}\right)^\theta \quad (2.1)$$

where $\varepsilon(x)$ is the strain at depth x from the eroded surface, ε_s is the failure rupture strain on the eroded surface, L is the thickness of the hardened layer, and θ is the shape factor of the power law.

After each cycle, the thickness of the hardened layer L and the surface strain ε_s will increase continuously until damage is initiated at the surface (ε_s reaches the failure rupture strain ε_R), at which point the strain profile is in steady-state.

$$\varepsilon_R = \varepsilon_{mean} \left(1 - \frac{\Delta L}{L + \Delta L}\right)^\theta \quad (2.2)$$

2.2 Correlative empirical methods

Empirical methods are common for addressing complex cavitation erosion, involving lab tests to correlate cavitation erosion resistance with mechanical properties.

1. Karimi and Leo

The Karimi and Leo phenomenological model describes cavitation erosion rate as a function of

Karimi and Leo

2. Noskievic

Noskievic formulated a mathematical relaxation model for the dynamics of the cavitation erosion using a differential equation applied to forced oscillations with damping:

$$\frac{d^2v}{dt^2} + 2\alpha \frac{dv}{dt} + \beta^2 v = I \quad (2.3)$$

where I is erosion intensity, which can vary linearly with time, $v = \frac{dv}{dt}$ is erosion rate, α is strain hardening or internal friction of material during plastic deformation, and β is coefficient inversely proportional to material strength. The general solution of equation can be written as:

$$v = af_0(\delta, \tau) + bf_1(\delta, \tau) \quad (2.4)$$

$$f_0(\delta, \tau) = \begin{cases} 1 - \exp(-\delta\tau) \left[\frac{\delta}{\omega} \sin(\omega\tau) + \cos(\omega\tau) \right] & \text{if } -1 < \delta < 1; \delta \neq 0 \\ 1 - \frac{1}{\delta_0^2 - 1} \left[\delta_0^2 \exp\left(-\frac{\tau}{\delta_0}\right) - \exp(-\delta_0\tau) \right] & \text{if } \delta > 1 \\ 1 - \cos(\tau) & \text{if } \delta = 0 \\ 1 - (1 + \tau) \exp(-\tau) & \text{if } \delta = 1 \end{cases}$$

$$f_1(\delta, \tau) = \begin{cases} 1 - \frac{2\delta}{\tau} [1 - \exp(-\delta\tau) [\cos\omega\tau + \varepsilon \sin\omega\tau]] & \text{if } -1 < \delta < 1; \delta \neq 0 \\ 1 - \frac{1}{\tau} \left(2\delta - \frac{1}{\delta_0(\delta_0^2 - 1)} \left[\exp(-\delta_0\tau) - \delta^4 \exp\left(-\frac{\tau}{\delta_0}\right) \right] \right) & \text{if } \delta > 1 \\ 1 - \frac{\sin(\tau)}{\tau} & \text{if } \delta = 0 \\ 1 - \frac{2[1 - \exp(-\tau)]}{\tau} + \exp(-\tau) & \text{if } \delta = 1 \end{cases}$$

$$\delta = \frac{\alpha}{\beta}, \quad \tau = \beta t, \quad \varepsilon = \frac{\delta^2 - 0.5}{\delta \sqrt{1 - \delta^2}}, \quad \omega = \sqrt{1 - \delta^2}, \quad \delta_0 = \delta + \sqrt{\delta^2 - 1}$$

3. Hoff and Langbein equation

Hoff and Langbein proposed a simple exponential function for the rate of erosion, representing the normalized erosion rate requiring only the A simple exponential function for the rate of erosion was proposed by Hoff and Langbein,

$$\frac{\dot{e}}{e_{\max}} = 1 - e^{-\frac{t_i}{t}}$$

\dot{e} - erosion rate at any time t e_{\max} - Maximum of peak erosion rate t_i - incubation period (intercept on time axis extended from linear portion of erosion-time curve) t - exposure time

4. L Sitnik model

$$V = V_o \left[\ln \left(\frac{t}{t_o} + 1 \right) \right]^\beta$$

$$\dot{V} = \frac{\beta V_o}{t + t_o} \left[\ln \left(\frac{t}{t_o} + 1 \right) \right]^{\beta - 1}$$

$$V_o > 0 \quad t_o > 0 \quad \beta \geq 1$$

Chapter 3

Experimental Investigations

3.1 Materials and Microstructure

The HIPed alloy was produced via canning the gas-atomized powders at 1200C and 100 MPa pressure for 4h, while the cast alloys were produced via sand casting. % Sieve analysis and description of powders

% Refer to Table of chemical compositions of both cast and HIPed alloys.

The microstructure of the alloys were observed via SEM in BSE mode, and the chemical compositions of the identified phases developed in the alloys were determined via EDS as well as with XRD under Cu K_{α} radiation.

Image analysis was also conducted to ascertain the volume fractions of individual phases.

The Vickers microhardness was measured using a Wilson hardness tester under loads of BLAH. Thirty measurements under each load were conducted on each sample.

Chapter 4

Discussion

4.1 Experimental Test Procedure

4.1.1 Hardness Tests

4.1.2 Cavitation

4.2 Relationships between cavitation erosion resistance and mechanical properties

4.3 Influence of vibratory amplitude

% Insert the whole spiel by that French dude about displacement and pressure (and then ruin it) The pressure of the solution depends on the amplitude of the vibratory tip attached to the ultrasonic device. Under simple assumptions, kinetic energy of cavitation is proportional to the square of the amplitude and maximum hammer pressure is proportional to A.

$$x = A \sin(2\pi ft) \quad (4.1)$$

$$v = \frac{dx}{dt} = 2\pi f A \cos(2\pi ft) \quad (4.2)$$

$$v_{max} = 2\pi f A \quad (4.3)$$

$$v_{mean} = \frac{1}{\pi} \int_0^\pi A \sin(2\pi ft) = 4fA \quad (4.4)$$

$$(4.5)$$

However, several researchers have found that erosion rates are not proportional to the second power of amplitude, but instead a smaller number. Thiruvengadam [37] and Hobbs find that erosion rates are proportional to the 1.8 and 1.5 power of peak-to-peak amplitude. Tomlinson et al find that erosion rate is linearly proportional to peak-to-peak amplitude in copper [3]. Maximum erosion rate is approximately proportional to the 1.5 power of p-p amplitude [4]. The propagation of ultrasonic waves may result in thermal energy absorption or into chemical energy, resulting in reduced power. For the purposes of converting data from studies that do not use an amplitude of 50um, a exponent factor of 1.5 has been applied.

References

- [1] R. Ahmed, H. L. de Villiers Lovelock, N. H. Faisal, and S. Davies, “Structure–property relationships in a CoCrMo alloy at micro and nano-scales,” *Tribology International*, vol. 80, pp. 98–114, Dec. 1, 2014, ISSN: 0301-679X. DOI: [10.1016/j.triboint.2014.06.015](https://doi.org/10.1016/j.triboint.2014.06.015). Accessed: Jun. 30, 2024. [Online]. Available: <https://www.sciencedirect.com/science/article/pii/S0301679X14002436>.
- [2] J.-C. Shin, J.-M. Doh, J.-K. Yoon, D.-Y. Lee, and J.-S. Kim, “Effect of molybdenum on the microstructure and wear resistance of cobalt-base Stellite hardfacing alloys,” *Surface and Coatings Technology*, vol. 166, no. 2, pp. 117–126, Mar. 24, 2003, ISSN: 0257-8972. DOI: [10.1016/S0257-8972\(02\)00853-8](https://doi.org/10.1016/S0257-8972(02)00853-8). Accessed: Mar. 5, 2025. [Online]. Available: <https://www.sciencedirect.com/science/article/pii/S0257897202008538>.
- [3] M. S. Hasan, A. M. Mazid, and R. Clegg, “The Basics of Stellites in Machining Perspective,” *International Journal of Engineering Materials and Manufacture*, vol. 1, no. 2, pp. 35–50, Dec. 19, 2016, ISSN: 0128-1852. DOI: [10.26776/ijemm.01.02.2016.01](https://doi.org/10.26776/ijemm.01.02.2016.01). Accessed: May 11, 2025. [Online]. Available: <https://deerhillpublishing.com/index.php/ijemm/article/view/13>.
- [4] U. Malayoglu and A. Neville, “Comparing the performance of HIPed and Cast Stellite 6 alloy in liquid–solid slurries,” *Wear*, 14th International Conference on Wear of Materials, vol. 255, no. 1, pp. 181–194, Aug. 1, 2003, ISSN: 0043-1648. DOI: [10.1016/S0043-1648\(03\)00287-4](https://doi.org/10.1016/S0043-1648(03)00287-4). Accessed: Feb. 17, 2025. [Online]. Available: <https://www.sciencedirect.com/science/article/pii/S0043164803002874>.
- [5] D. Raghu and J. B. C. Wu, “Recent Developments in Wear and Corrosion Resistant Alloys for Oil Industry,” presented at the CORROSION 1997, Association for Materials Protection and Performance, Mar. 9, 1997, pp. 1–20. DOI: [10.5006/C1997-97016](https://doi.org/10.5006/C1997-97016). Accessed: May 12, 2025. [Online]. Available: <https://dx.doi.org/10.5006/C1997-97016>.
- [6] R. Ahmed, A. Fardan, and S. Davies, “Mapping the mechanical properties of cobalt-based stellite alloys manufactured via blending,” *Advances in Materials and Processing Technologies*, vol. 0, no. 0, pp. 1–30, Jun. 2, 2023, ISSN: 2374-068X. DOI: [10.1080/2374068X.2023.2220242](https://doi.org/10.1080/2374068X.2023.2220242). Accessed: Jul. 13, 2024. [Online]. Available: <https://doi.org/10.1080/2374068X.2023.2220242>.

- [7] M. Alimardani, V. Fallah, A. Khajepour, and E. Toyserkani, "The effect of localized dynamic surface preheating in laser cladding of Stellite 1," *Surface and Coatings Technology*, vol. 204, no. 23, pp. 3911–3919, Aug. 25, 2010, ISSN: 0257-8972. DOI: [10.1016/j.surfcoat.2010.05.009](https://doi.org/10.1016/j.surfcoat.2010.05.009). Accessed: Mar. 31, 2025. [Online]. Available: <https://www.sciencedirect.com/science/article/pii/S0257897210003701>.
- [8] M. Ashworth, M. Jacobs, and S. Davies, "Microstructure and property relationships in HIPped Stellite powders," *Powder Metallurgy*, vol. 42, no. 3, pp. 243–249, Mar. 1, 1999, ISSN: 0032-5899. DOI: [10.1179/003258999665585](https://doi.org/10.1179/003258999665585). Accessed: Apr. 3, 2025. [Online]. Available: <https://journals.sagepub.com/action/showAbstract>.
- [9] P. O. Bunch, M. P. Hartmann, and T. A. Bednarowicz, "Corrosion/Galling Resistant Hardfacing Materials for Offshore Production Valves," presented at the Offshore Technology Conference, OnePetro, May 1, 1989. DOI: [10.4043/6070-MS](https://doi.org/10.4043/6070-MS). Accessed: Apr. 1, 2025. [Online]. Available: <https://dx.doi.org/10.4043/6070-MS>.
- [10] J. Davis and A. Committee, *Nickel, Cobalt, and Their Alloys* (ASM Specialty Handbook). ASM International, 2000, ISBN: 978-0-87170-685-0. [Online]. Available: <https://books.google.ae/books?id=IePhmnbmRWkC>.
- [11] V. M. Desai, C. M. Rao, T. H. Kosel, and N. F. Fiore, "Effect of carbide size on the abrasion of cobalt-base powder metallurgy alloys," *Wear*, vol. 94, no. 1, pp. 89–101, Feb. 15, 1984, ISSN: 0043-1648. DOI: [10.1016/0043-1648\(84\)90168-6](https://doi.org/10.1016/0043-1648(84)90168-6). Accessed: Nov. 17, 2024. [Online]. Available: <https://www.sciencedirect.com/science/article/pii/0043164884901686>.
- [12] M. M. Ferozhkhan, K. G. Kumar, and R. Ravibharath, "Metallurgical Study of Stellite 6 Cladding on 309-16L Stainless Steel," *Arabian Journal for Science and Engineering*, vol. 42, no. 5, pp. 2067–2074, May 1, 2017, ISSN: 2191-4281. DOI: [10.1007/s13369-017-2457-7](https://doi.org/10.1007/s13369-017-2457-7). Accessed: Mar. 31, 2025. [Online]. Available: <https://doi.org/10.1007/s13369-017-2457-7>.
- [13] W. Pacquentin, P. Wident, J. Varlet, T. Cailloux, and H. Maskrot, "Temperature influence on the repair of a hardfacing coating using laser metal deposition and assessment of the repair innocuity," *Journal of Advanced Joining Processes*, vol. 11, p. 100 284, Jun. 1, 2025, ISSN: 2666-3309. DOI: [10.1016/j.jajp.2025.100284](https://doi.org/10.1016/j.jajp.2025.100284). Accessed: Mar. 31, 2025. [Online]. Available: <https://www.sciencedirect.com/science/article/pii/S2666330925000056>.
- [14] V. L. Ratia, D. Zhang, M. J. Carrington, J. L. Daure, D. G. McCartney, P. H. Shipway, and D. A. Stewart, "Comparison of the sliding wear behaviour of self-mated HIPed Stellite 3

- and Stellite 6 in a simulated PWR water environment,” *Wear*, 22nd International Conference on Wear of Materials, vol. 426–427, pp. 1222–1232, Apr. 30, 2019, ISSN: 0043-1648. DOI: [10.1016/j.wear.2019.01.116](https://doi.org/10.1016/j.wear.2019.01.116). Accessed: Jun. 30, 2024. [Online]. Available: <https://www.sciencedirect.com/science/article/pii/S004316481930211X>.
- [15] K. Zhang and L. Battiston, “Friction and wear characterization of some cobalt- and iron-based superalloys in zinc alloy baths,” *Wear*, vol. 252, no. 3, pp. 332–344, Feb. 1, 2002, ISSN: 0043-1648. DOI: [10.1016/S0043-1648\(01\)00889-4](https://doi.org/10.1016/S0043-1648(01)00889-4). Accessed: Apr. 1, 2025. [Online]. Available: <https://www.sciencedirect.com/science/article/pii/S0043164801008894>.
- [16] R. Ahmed, H. L. de Villiers Lovelock, and S. Davies, “Sliding wear of blended cobalt based alloys,” *Wear*, vol. 466–467, p. 203 533, Feb. 15, 2021, ISSN: 0043-1648. DOI: [10.1016/j.wear.2020.203533](https://doi.org/10.1016/j.wear.2020.203533). Accessed: Jul. 13, 2024. [Online]. Available: <https://www.sciencedirect.com/science/article/pii/S0043164820309923>.
- [17] P. Crook, “Cobalt-base alloys resist wear, corrosion, and heat,” *Cobalt-base alloys resist wear, corrosion, and heat*, vol. 145, no. 4, pp. 27–30, 1994, ISSN: 0882-7958.
- [18] A. Frenk and W. Kurz, “Microstructural effects on the sliding wear resistance of a cobalt-based alloy,” *Wear*, vol. 174, no. 1, pp. 81–91, May 1, 1994, ISSN: 0043-1648. DOI: [10.1016/0043-1648\(94\)90089-2](https://doi.org/10.1016/0043-1648(94)90089-2). Accessed: Feb. 18, 2025. [Online]. Available: <https://www.sciencedirect.com/science/article/pii/0043164894900892>.
- [19] A. S. Kurlov and A. I. Gusev, “Phase equilibria in the W–C system and tungsten carbides,” *Russian Chemical Reviews*, vol. 75, no. 7, pp. 617–636, Jul. 31, 2006, ISSN: 0036-021X, 1468-4837. DOI: [10.1070/RC2006v075n07ABEH003606](https://doi.org/10.1070/RC2006v075n07ABEH003606). Accessed: May 11, 2025. [Online]. Available: <https://iopscience.iop.org/article/10.1070/RC2006v075n07ABEH003606>.
- [20] W. H. Jiang, X. D. Yao, H. R. Guan, and Z. Q. Hu, “Secondary M₆C Precipitation in a Cobalt–base Superalloy,” *Journal of Materials Science Letters*, vol. 18, no. 4, pp. 303–305, Feb. 1, 1999, ISSN: 1573-4811. DOI: [10.1023/A:1006627122234](https://doi.org/10.1023/A:1006627122234). Accessed: May 12, 2025. [Online]. Available: <https://doi.org/10.1023/A:1006627122234>.
- [21] M. Mohammadnezhad, V. Javaheri, M. Shamanian, S. Rizaneh, and J. A. Szpunar, “Insight to the Microstructure Characterization of a HP Austenitic Heat Resistant Steel after Long-term Service Exposure,”
- [22] K. C. Antony, “Wear-Resistant Cobalt-Base Alloys,” *JOM*, vol. 35, no. 2, pp. 52–60, Feb. 1, 1983, ISSN: 1543-1851. DOI: [10.1007/BF03338205](https://doi.org/10.1007/BF03338205). Accessed: Jul. 13, 2024. [Online]. Available: <https://doi.org/10.1007/BF03338205>.

- [23] N. S. McIntyre, D. Zetaruk, and E. V. Murphy, "X-Ray photoelectron spectroscopic study of the aqueous oxidation of stellite-6 alloy," *Surface and Interface Analysis*, vol. 1, no. 4, pp. 105–110, 1979, ISSN: 1096-9918. DOI: [10.1002/sia.740010402](https://doi.org/10.1002/sia.740010402). Accessed: May 11, 2025. [Online]. Available: <https://onlinelibrary.wiley.com/doi/abs/10.1002/sia.740010402>.
- [24] Z. Česánek, J. Schubert, Š. Houdková, O. Bláhová, and M. Prantnerová, "Deterioration of Local Mechanical Properties of HVOF-Sprayed Stellite 6 after Exposure to High-Temperature Corrosion," *Key Engineering Materials*, vol. 662, pp. 115–118, 2015, ISSN: 1662-9795. DOI: [10.4028/www.scientific.net/KEM.662.115](https://doi.org/10.4028/www.scientific.net/KEM.662.115). Accessed: May 11, 2025. [Online]. Available: <https://www.scientific.net/KEM.662.115>.
- [25] C. J. Heathcock, A. Ball, and B. E. Protheroe, "Cavitation erosion of cobalt-based Stellite® alloys, cemented carbides and surface-treated low alloy steels," *Wear*, vol. 74, no. 1, pp. 11–26, Dec. 8, 1981, ISSN: 0043-1648. DOI: [10.1016/0043-1648\(81\)90191-5](https://doi.org/10.1016/0043-1648(81)90191-5). Accessed: Feb. 5, 2025. [Online]. Available: <https://www.sciencedirect.com/science/article/pii/0043164881901915>.
- [26] "Cavitation Erosion," in *Fundamentals of Cavitation*, J.-P. Franc and J.-M. Michel, Eds., Dordrecht: Springer Netherlands, 2005, pp. 265–291, ISBN: 978-1-4020-2233-3. DOI: [10.1007/1-4020-2233-6_12](https://doi.org/10.1007/1-4020-2233-6_12). Accessed: Apr. 13, 2025. [Online]. Available: https://doi.org/10.1007/1-4020-2233-6_12.
- [27] S. Romo, J. Santa, J. Giraldo, and A. Toro, "Cavitation and high-velocity slurry erosion resistance of welded Stellite 6 alloy," *Tribology International*, vol. 47, pp. 16–24, 2012, ISSN: 0301679X (ISSN). DOI: [10.1016/j.triboint.2011.10.003](https://doi.org/10.1016/j.triboint.2011.10.003). [Online]. Available: <https://www.scopus.com/inward/record.uri?eid=2-s2.0-84856240362&doi=10.1016%2fj.triboint.2011.10.003&partnerID=40&md5=77bc5b529937543083c683cc6f5d689d>.
- [28] M. T. Gevari, T. Abbasiasl, S. Niazi, M. Ghorbani, and A. Koşar, "Direct and indirect thermal applications of hydrodynamic and acoustic cavitation: A review," *Applied Thermal Engineering*, vol. 171, p. 115 065, May 5, 2020, ISSN: 1359-4311. DOI: [10.1016/j.applthermaleng.2020.115065](https://doi.org/10.1016/j.applthermaleng.2020.115065). Accessed: Apr. 13, 2025. [Online]. Available: <https://www.sciencedirect.com/science/article/pii/S135943111937766X>.
- [29] Z. Huang, B. Wang, F. Liu, M. Song, S. Ni, and S. Liu, "Microstructure evolution, martensite transformation and mechanical properties of heat treated Co-Cr-Mo-W alloys by selective laser melting," *International Journal of Refractory Metals and Hard Materials*, vol. 113, p. 106 170, Jun. 1, 2023, ISSN: 0263-4368. DOI: [10.1016/j.ijrmhm.2023.106170](https://doi.org/10.1016/j.ijrmhm.2023.106170). Accessed: Apr. 13, 2025. [Online]. Available: <https://www.sciencedirect.com/science/article/pii/S0263436823000707>.

- [30] H. M. Tawancy, V. R. Ishwar, and B. E. Lewis, "On the fcc \rightarrow hcp transformation in a cobalt-base superalloy (Haynes alloy No. 25)," *Journal of Materials Science Letters*, vol. 5, no. 3, pp. 337–341, Mar. 1, 1986, ISSN: 1573-4811. DOI: [10.1007/BF01748098](https://doi.org/10.1007/BF01748098). Accessed: Apr. 13, 2025. [Online]. Available: <https://doi.org/10.1007/BF01748098>.
- [31] H. Yu, R. Ahmed, and H. de Villiers Lovelock, "A Comparison of the Tribo-Mechanical Properties of a Wear Resistant Cobalt-Based Alloy Produced by Different Manufacturing Processes," *Journal of Tribology*, vol. 129, no. 3, pp. 586–594, Jan. 9, 2007, ISSN: 0742-4787. DOI: [10.1115/1.2736450](https://doi.org/10.1115/1.2736450). Accessed: Nov. 17, 2024. [Online]. Available: <https://doi.org/10.1115/1.2736450>.
- [32] V. Stoica, R. Ahmed, and T. Itsukaichi, "Influence of heat-treatment on the sliding wear of thermal spray cermet coatings," *Surface and Coatings Technology*, vol. 199, no. 1, pp. 7–21, 2005, ISSN: 02578972 (ISSN). DOI: [10.1016/j.surfcoat.2005.03.026](https://www.sciencedirect.com/science/article/pii/S02578972(05)00026-6). [Online]. Available: <https://www.scopus.com/inward/record.uri?eid=2-s2.0-21844464044&doi=10.1016%2fj.surfcoat.2005.03.026&partnerID=40&md5=6ad736723e828d39edf4a37c5975d2dc>.
- [33] R. Ahmed, H. L. de Villiers Lovelock, S. Davies, and N. H. Faisal, "Influence of Re-HIPing on the structure–property relationships of cobalt-based alloys," *Tribology International*, vol. 57, pp. 8–21, Jan. 1, 2013, ISSN: 0301-679X. DOI: [10.1016/j.triboint.2012.06.025](https://www.sciencedirect.com/science/article/pii/S0301679X12002241). Accessed: Jun. 30, 2024. [Online]. Available: <https://www.sciencedirect.com/science/article/pii/S0301679X12002241>.
- [34] H. Yu, R. Ahmed, H. d. V. Lovelock, and S. Davies, "Influence of Manufacturing Process and Alloying Element Content on the Tribomechanical Properties of Cobalt-Based Alloys," *Journal of Tribology*, vol. 131, no. 011601, Dec. 4, 2008, ISSN: 0742-4787. DOI: [10.1115/1.2991122](https://doi.org/10.1115/1.2991122). Accessed: May 1, 2025. [Online]. Available: <https://doi.org/10.1115/1.2991122>.
- [35] M. Szala, D. Chocyk, A. Skic, M. Kamiński, W. Macek, and M. Turek, "Effect of nitrogen ion implantation on the cavitation erosion resistance and cobalt-based solid solution phase transformations of HIPed stellite 6," *Materials*, vol. 14, no. 9, 2021, ISSN: 19961944 (ISSN). DOI: [10.3390/ma14092324](https://www.sciencedirect.com/science/article/pii/S1996194421001944). [Online]. Available: <https://www.scopus.com/inward/record.uri?eid=2-s2.0-85105941706&doi=10.3390%2fma14092324&partnerID=40&md5=4c846be7d06977d42697c88c326e5923>.
- [36] A. Świetlicki, M. Szala, and M. Walczak, "Effects of Shot Peening and Cavitation Peening on Properties of Surface Layer of Metallic Materials—A Short Review," *Materials*, vol. 15, no. 7, p. 2476, 7 Jan. 2022, ISSN: 1996-1944. DOI: [10.3390/ma15072476](https://www.mdpi.com/1996-1944/15/7/2476). Accessed: May 12, 2025. [Online]. Available: <https://www.mdpi.com/1996-1944/15/7/2476>.

- [37] A. Thiruvengadam, "Theory of erosion," *Proc. 2nd Meersburg Conf. on Rain Erosion and Allied Phenomena*, vol. 2, p. 53, Mar. 1, 1967.